^{41}K(^{3}He, t) reaction at 25 MeV†

M. Stautberg Greenwood and M. Pluta
De Paul University, Chicago, Illinois 60614
and Argonne National Laboratory, Argonne, Illinois 60439

L. R. Greenwood
Northwestern University, Evanston, Illinois 60201
and Argonne National Laboratory, Argonne, Illinois 60439

N. Anantaraman*
Argonne National Laboratory, Argonne, Illinois 60439

(Received 26 August 1974)

Angular distributions for the ^{41}K(^{3}He, t)^{41}Ca reaction were measured for 35 states up to 7.61-MeV excitation energy in ^{41}Ca. L values were deduced from a microscopic distorted-wave Born-approximation analysis. Of especial interest was the comparison of $T_<$ and $T_>$ states with the same shell-model configurations. The $\frac{7}{2}^-$ ground state and $\frac{7}{2}^-$ excited analog state at 7.12 MeV were both fitted by $L=3+5$, although the data exhibited more structure and peaked at a more forward angle than the DW calculation. Whereas the angular distribution of the $\frac{3}{2}^+$ analog state at 5.822 MeV was described principally by $L=0$, the angular distribution of the $\frac{3}{2}^+$ antianalog state at 2.005 MeV was fitted by $L=2$. Evidence is presented to show that the $L=2$ character of the angular distribution of the antianalog state is due to the $f_{7/2}\rightarrow f_{7/2}$ transition with $L=2$, $S=0$. The 2.68- and 3.394-MeV states with $J^\pi=\frac{1}{2}^+$, excited by $l_n=0$ in ^{42}Ca(p, d), can be obtained by either $f_{7/2}\rightarrow f_{7/2}$ or $s_{1/2}\rightarrow d_{3/2}$ transitions, both with $L=2$, $S=0$. However, the 2.68-MeV state was not observed, suggesting that the effects of the two competing transitions enhance the 3.394-MeV state but may tend to cancel for the 2.68-MeV state. The 4.098-MeV state ($J^\pi=\frac{5}{2}^+$) was strongly excited and appears to arise from the $f_{7/2}\rightarrow f_{7/2}$ transition with $L=2$ and $S=0$ or 1. The transition to the 2.875-MeV level, known to have $l_n=4$ in ^{40}Ca(d, p), was assigned $L=2$, thus strongly suggesting $J^\pi=\frac{7}{2}^+$ since spin-flip excitation is expected to be weak.

[NUCLEAR REACTIONS ^{41}K(^{3}He, t), $E=25$ MeV; measured $\sigma(\theta)$. Enriched targets, DWBA analysis. ^{41}Ca deduced levels, l, π, IAS.]

I. INTRODUCTION

The apparent complexity of the (^{3}He, t) charge-exchange reaction mechanism has led to many difficulties in attempts to describe these reactions by microscopic distorted-wave Born-approximation (DWBA) calculations. In particular, the calculations fail to adequately describe the angular distributions to $T_<$ states, especially at forward angles, which makes it difficult to extract spectroscopic information.[1] Presumably, these difficulties are due to the presence of two-step reaction mechanisms such as formation of an intermediate α-particle cluster followed by stripping. The purpose of the present study was to simultaneously investigate the charge-exchange reaction to $T_>$ and $T_<$ states involving the same shell-model orbitals, as would be the case in the ^{41}K(^{3}He, t)-^{41}Ca reaction. Also, the wealth of information already gathered about ^{41}Ca from a variety of reactions,[2-7] greatly facilitates interpretation of the ^{41}K(^{3}He, t)^{41}Ca reaction. Schwartz and Watson[8] have studied the ^{41}K(^{3}He, t) reaction observing the strength of the cross shell transitions.

The shell-model configurations of ^{41}K and ^{41}Ca are shown in Fig. 1. Since the ^{41}K ground state has $T=\frac{3}{2}$, the isospin must be lowered by one unit to make the $T=\frac{1}{2}$ ^{41}Ca ground state. This involves the replacement of a $f_{7/2}$ neutron by a $d_{3/2}$ proton. Other $T_<=\frac{1}{2}$ states involve more complicated transfers, as will be discussed in detail later.

The $T_>=\frac{3}{2}$ analog of the ^{41}K ground state has been identified in ^{41}Ca at 5.813 MeV.[3] The $\frac{7}{2}^-$ state at 1.29 MeV in ^{41}K corresponds to the excitation of a $d_{3/2}$ nucleon into the $f_{7/2}$ orbital,[9] which results in the $(d_{3/2})^6(f_{7/2})^3$ configuration. The analogous configuration in ^{41}Ca can thus be easily reached by replacement of a $d_{3/2}$ neutron by an $f_{7/2}$ proton. This $\frac{7}{2}^-$ excited analog state, which is expected to have an energy of $5.813+1.29=7.10$ MeV, has been identified at 7.13 ± 0.05 MeV in the ^{42}Ca(p, d) reaction[4] and at 7.173 MeV in the ^{42}Ca(^{3}He, α) reaction.[5]

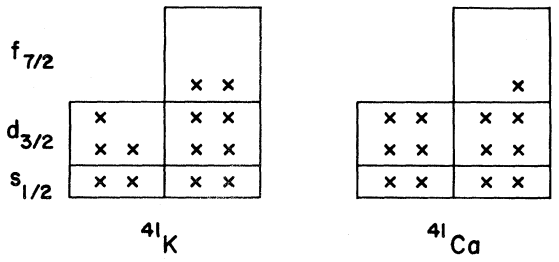

FIG. 1. The ^{41}K and ^{41}Ca ground state configuration.

Thus, the present study allows the comparison of the angular distribution from the (^{3}He, t) reaction to the $T_<$ ground state with that to the $T_>$ excited analog state, both of which have $J^\pi = \frac{7}{2}^-$ and involve the same $d_{3/2}$ and $f_{7/2}$ shell-model orbitals. This comparison was feasible because of the development of a position-sensitive proportional counter.[10]

Several reports[11,12] comparing the (^{3}He, t) angular distributions to the analog state and the antianalog state have indicated an anomalous behavior for the antianalog state. In the study of Hinrichs *et al.*[11] the angular distributions of the 0^+ analog states have $L=0$, while the angular distributions of 0^+ antianalog states have an empirical $L=1$ shape even though $L=1$ is not permitted. This effect can be explained by considering a pickup-stripping mechanism for the (^{3}He, t) reaction.[13,14] The $\frac{3}{2}^+$ antianalog state has been identified[15] at 2.010 MeV in ^{41}Ca. Thus, the present study also affords a comparison of the angular distributions which lead to the analog and antianalog states.

II. EXPERIMENTAL PROCEDURES

A beam of 25-MeV ^{3}He particles was obtained from the Argonne National Laboratory FN tandem Van de Graaff accelerator. The reaction products were detected by placing either Kodak NTB emulsions or a position-sensitive proportional counter in the focal plane of the split-pole magnetic spectrograph. The targets, kept in a vacuum at all times, were obtained by evaporating potassium iodide enriched to 99.2% ^{41}K onto 30-μg/cm^2 carbon backings. A silicon-surface-barrier detector measuring the elastic scattering from iodine, was placed at 30 or 60° in the scattering chamber to monitor target thickness changes. The elastic scattering measurements from iodine were used to calculate the target thickness. According to optical-model calculations, the elastic scattering at 30° is 97% of Rutherford scattering. The thickness of the targets ranged from 50 to 100 μg/cm^2 of potassium.

Initially, the tritons were analyzed by an Enge spectrograph and recorded on nuclear emulsions. However, the lower energy triton groups were completely lost in the high background of the competing ^{41}K(^{3}He, d)^{42}Ca reaction. Fortunately, a position-sensitive proportional counter,[10] which was also under development, became available during the experiment. The counter was able to identify particles by their energy loss, thus allowing the separation of tritons from the intense deuteron background for the $\frac{7}{2}^-$ excited analog state as well as a large uninvestigated region of high excitation in ^{41}Ca.

A. Emulsions

A sample spectrum obtained using emulsions is shown in Fig. 2. The tracks on the plates were counted using a computer-controlled plate scanner. The computer code QPLOT[16] was used to obtain plots of counts versus Q value in order to identify

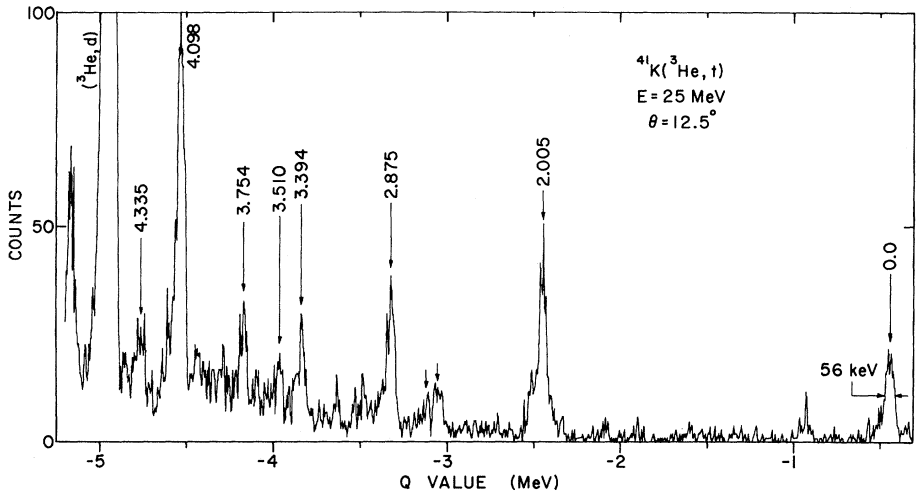

FIG. 2. Spectrum obtained using emulsions. The two arrows show traces of peaks at 2.60 and 2.68 MeV.

excited states in ^{41}Ca. Also shown in Fig. 2 is the deuteron peak from the ^{41}K(^{3}He, d)^{42}Ca$_{g.s.}$ reaction. Due to the location of this peak and the Q values of other reactions as well, only tritons are found over a large distance making the use of emulsions very feasible. Since the triton peaks were well separated, the yields were obtained by summing the counts in the peaks. Error in the yields included statistical uncertainty, as well as errors in determining the background and setting the limits of the peaks.

B. Position-sensitive proportional counter

The tritons to states above 4.5-MeV excitation in ^{41}Ca were analyzed using a 50-cm position-sensitive proportional counter system[10] in the focal plane of an Enge spectrograph. Since the (^{3}He, d) reaction produces a high flux of deuterons with the same magnetic rigidity as the tritons of interest, the experiment would not have been possible with conventional nuclear emulsions. The counter system was able to identify particles by their energy loss as well as their position on the focal plane.

The detector system consisted of two separate detectors: a thin (6 mm) counter with a single high-resistance (2 $k\Omega$/mm) anode followed by a thick (5 cm) ordinary proportional counter. The thin counter is used to obtain high resolution [~1 mm, full width at half-maximum (FWHM)] position information, whereas the thick counter is used to measure the energy lost by the particle [$\Delta E \sim (5-10)\%$, FWHM]. Both counters are mounted in a large vacuum-tight box. Mylar foils (0.15–0.5 mil) are used for the box window and to define the counter volumes. The entire box is filled with argon (90%) and methane (10%) at a usual pressure of 1 atm.

Particle position was determined by measuring the difference in risetime between pulses arriving

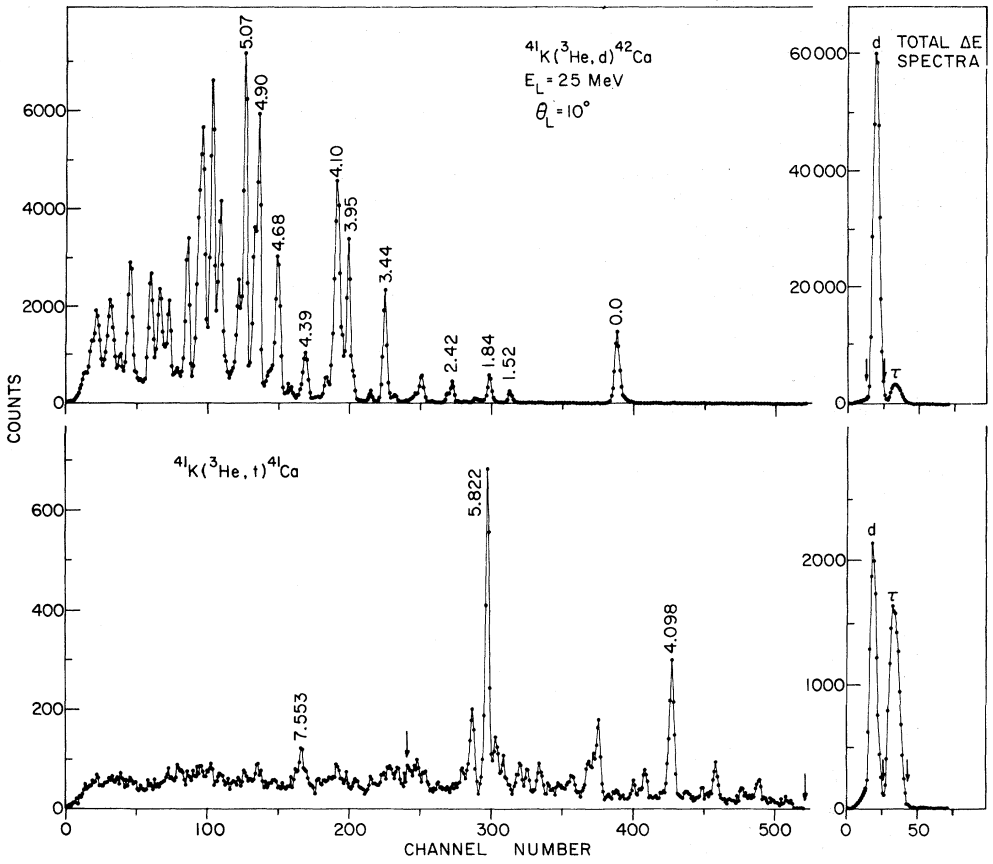

FIG. 3. Spectra for the ^{41}K(^{3}He, t)^{41}Ca and ^{41}K(^{3}He, d)^{42}Ca reactions at 25 MeV taken with the position-sensitive proportional counter. The top panel shows the deuteron spectrum obtained by "light penning" the ΔE spectrum as indicated by the arrows. Similarly, the bottom panel shows the triton spectrum. The bottom ΔE spectrum was obtained by light penning the position spectrum as shown to emphasize the triton peak by reducing the intensity of deuterons.

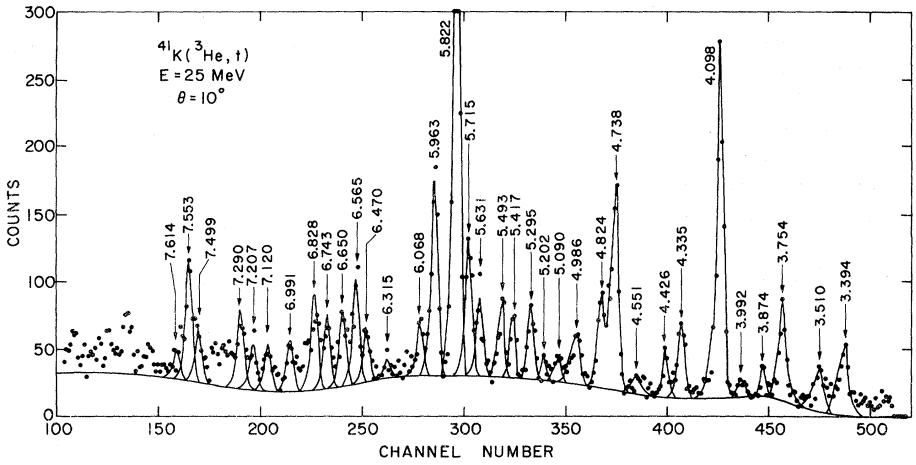

FIG. 4. Triton spectrum obtained using position-sensitive proportional counter and analysis from program AUTOFIT.

at each end of the anode. The pulses are converted to bipolar pulses with filter amplifiers ($\tau = 5$ μs) and time signals are obtained from crossover detectors. This method assures good linearity ($\leq 1\%$) and high spatial resolution (~50 ns/mm). The crossover signals are then used to start and stop a time-to-amplitude converter (TAC).

The position TAC and energy loss (ΔE) signals are then stored in coincidence. This coincidence condition between the two independent counters has an additional bonus in that γ, neutron, or noise pulses are almost entirely eliminated. An array of 512×64 channels was used and the entire array was stored on magnetic tape for subsequent analysis. One-dimensional x and y projections can be simultaneously displayed or analyzed "on-line" using a light-pen facility. This feature is very useful in allowing the user to examine the experiment in progress, which is something that cannot be done with nuclear emulsions. This was very important in the present experiment since the cross sections were very small.

Sample spectra, demonstrating the counter performance, are shown in Fig. 3. Both the position and ΔE resolution were limited in the present experiment by the large spectrograph aperture (3.3 msr) and energy spread caused by the target. Further, the ΔE resolution is worsened by the fact that a particle striking one end of the counter loses more energy than those at the opposite end due to the difference in particle energy. Further, the ΔE resolution may be enhanced by looking at only part of the position spectra, as shown in Fig. 3. The ΔE resolution was sufficient to completely resolve deuterons from tritons.

The position spectra were calibrated by using known peak positions to determine the relationship between channel number and focal plane distance. The resultant curve of position vs channel number was then fitted by an eighth-order polynomial, which was then used in the standard plate analysis program QPLOT[16] to determine Q values. The triton spectrum was analyzed using program AUTOFIT,[16] and sample is shown in Fig. 4. The results of the AUTOFIT analyses were then used to obtain angular distributions.

III. RESULTS AND DISCUSSION

The angular distributions were compared with DW calculations obtained from the program DWUCK.[17] A microscopic form factor was used, which arises from the interaction between a target neutron and a proton in the ^{3}He projectile. A Yukawa potential was used for this interaction. The ^{3}He and triton optical-model parameters[18, 19] are listed in Table I. The single-particle wave functions were calculated with a radius of $1.25A^{1/3}$ fm and a diffuseness of 0.65 fm. The effects of varying the reciprocal range parameter α and the optical-model parameters are shown in Fig. 5. Calculations were carried out using the optical-model parameters in Table I for the $f_{7/2} \rightarrow f_{7/2}$ transition with $L = 2$ and 4 and for the $f_{7/2} \rightarrow d_{3/2}$ transition with $L = 3$ and 5 for $\alpha = 0.5$, 0.7, 1.0, and 1.4

TABLE I. Optical-model parameters.

	V_R (MeV)	r_R (fm)	a_R (fm)	V_I [a] (MeV)	r_I (fm)	a_I (fm)
^{41}K + ^{3}He [b]	176.9	1.14	0.723	14.5	1.64	0.910
^{41}Ca + t [c]	149.0	1.24	0.671	18.8	1.57	0.776

[a] Indicates a volume potential.
[b] Reference 18.
[c] Reference 19.

fm^{-1}. The results for $L=2$, 3, and 5, shown in Figs. 5(a)–5(c), demonstrate that the angular position of the first maximum is dependent upon the value of α. $L=2$ is the least affected. The effects for $L=4$ are very similar to those for $L=3$ and 5. However, the results do show that it is possible to determine the angular momentum transfer L by comparing an experimental angular distribution with distorted-wave calculations. Unless noted, the experimental angular distributions are compared with distorted-wave calculations with $\alpha=1.0$ fm^{-1}. The effects of varying the optical-model parameters are shown in Fig. 5(d) for $L=2$, where the ^{3}He optical-model parameters are used in the ingoing and outgoing channels (labeled ^{3}He-^{3}He) and the triton parameters are used in both channels (labeled t-t). The angular positions of the first and second maxima are not affected at all by the variation in optical model parameters. Similar results were found for $L=3$, 4, and 5.

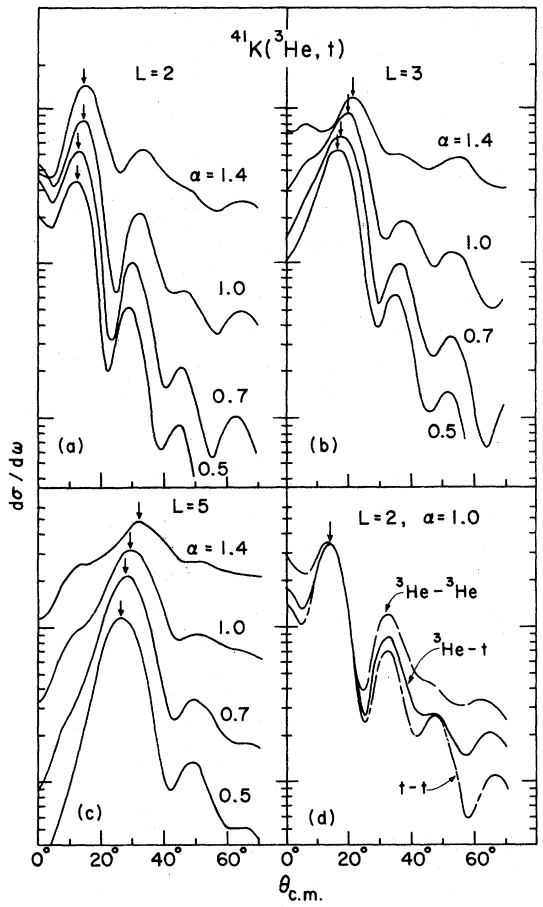

FIG. 5. The placement of the DW calculations, plotted on a semilogarithmic scale, allows comparison of the curves, but does not indicate the relative magnitude of the angular distributions. The effects of varying the reciprocal range parameter are shown in Figs. 5(a)–5(c) using the optical-model parameter listed in Table I. The effects of varying the optical-model parameters are shown in Fig. 5(d), where $\alpha=1.0$ fm^{-1}. The curve labeled ^{3}He-t indicates that the parameters listed in Table I were used. The curve labeled ^{3}He-^{3}He indicates that the ^{3}He parameters of Table I were used in both the ingoing and outgoing DW channels and the curve labeled t-t indicates that the triton parameters of Table I were used in both channels. Arrows are shown to emphasize the location of the maxima.

A. Comparison of the ^{41}Ca ground state and excited analog state

In the present study the $\frac{7}{2}^{-}$ excited analog state was identified at 7.120 ± 0.011 MeV. This energy agrees with the value of 7.13 ± 0.011 MeV reported in ^{42}Ca(p,d).[4] A higher value of 7.173 MeV was reported in ^{42}Ca(^{3}He, α),[5] however, they also report 5.852 MeV for the ground state analog, which

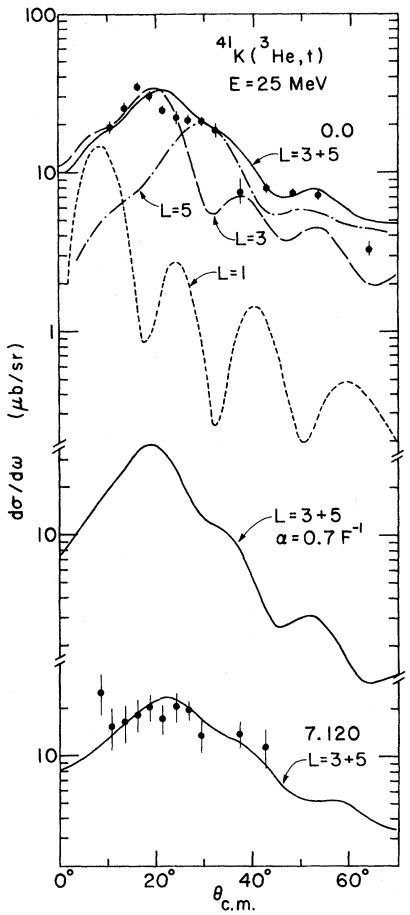

FIG. 6. Comparison of the ground-state and 7.12-MeV angular distributions with DW calculations. The $L=1$ curve is displaced for clarity. Except where noted, $\alpha=1$ fm^{-1}.

is 40 keV higher than found in more accurate γ-decay studies,[3] suggesting a systematic error.

As discussed in the Introduction, the excitation of the $\frac{7}{2}^-$ ground state and the excited analog state involve the $d_{3/2}$ and $f_{7/2}$ orbitals. Therefore, only angular momentum transfers $L=1$, 3, and 5 are permitted. Since ^{41}K has $J^\pi=\frac{3}{2}^+$, $L=1$ must be accompanied by spin-flip $S=1$, which is expected to be weak.

In Fig. 6 the ground state angular distribution is compared with DW calculations for $L=1$, 3, and 5. Calculations show that including a tensor force does not alter the $L=1$ characteristic shape. It is evident that the angular distribution is characterized by a combination of $L=3$ and 5. An $L=5$ contribution is necessary to fit the data in the region of 30°. The effect of $L=1$ would be most evident at angles less than 10° for which data were not taken. However, spin-flip contributions are known to be much weaker than non-spin-flip contributions.[20,21] The curve which best fits the data points is the result of including $L=3$ and $L=5$ contributions. While this curve does represent the trend of the data, it does not give an accurate fit at forward angles. It has been observed in many (^{3}He, t) reactions[1] that DW calculations cannot produce a peak at as small a forward angle as the experimental data. In the present case, the ground state distribution peaks at about 16°, whereas the DW calculation peaks at about 21°. The fit at angles between 10 and 25° can be improved by using DW calculations with $\alpha=0.7$ fm^{-1} as shown in Fig. 6. However, the fit for angles greater than 25° is poor.

The angular distribution of the 7.120-MeV state, also shown in Fig. 6, is also compared with a DW calculation that includes $L=3$ and $L=5$ contributions. The fit is similar to that obtained for the ground state, although the errors are much larger.

B. Ground-state analog and the antianalog state

The ground-state configuration of ^{41}K is shown in Fig. 1. The analog state in ^{41}Ca is obtained by replacing a $d_{3/2}$ or an $f_{7/2}$ neutron by a proton in the same orbit. Thus, both the ^{41}K ground state and the ^{41}Ca analog state have the following configuration

$$[d_{3/2}{}^{-1}(\tfrac{3}{2},\tfrac{1}{2})f_{7/2}{}^2(0,1)]_{(J,T)},$$

where $J=\frac{3}{2}$ and $T=\frac{3}{2}$. The numbers in parentheses indicate the angular momentum and isospin coupling. The antianalog state has the same configuration, but $T=\frac{1}{2}$. The analog and antianalog states have been identified[3,4] at 5.822 and 2.005 MeV, respectively. Since both states have $J^\pi=\frac{3}{2}^+$, only $L=0$ and 2 are permitted. DW calculations show that the predicted cross section for $L=0$ is about 3 times larger than for $L=2$ at 20°. Thus, both the analog and antianalog states are expected to have predominantly $L=0$ angular distributions. However, the data in Fig. 7 show the surprising result that the angular distribution of the analog state is characterized by $L=0$, while the antianalog state is characterized by $L=2$. The work of French and Macfarlane[22] may be used to interpret this result. They calculated the matrix element of the charge-exchange operator for target nuclei in which there were two unfilled proton subshells. The results show that the excitation of the analog state is expected to be very strong due to the addition of two terms (one for each subshell), while the antianalog may be very weak due to the subtraction of two terms. Since the antianalog state is not excited with $L=0$, this is strong evidence that such a cancellation does indeed occur. Perhaps the excitation of this state in the (^{3}He, t) reaction is due to another shell-model configuration which is mixed with the antianalog configuration. One possibility is the $[d_{3/2}{}^{-1}(\frac{3}{2},\frac{1}{2})f_{7/2}{}^2(1,0)]_{(3/2,\,1/2)}$ configuration, which can be reached by $L=0$ or 2

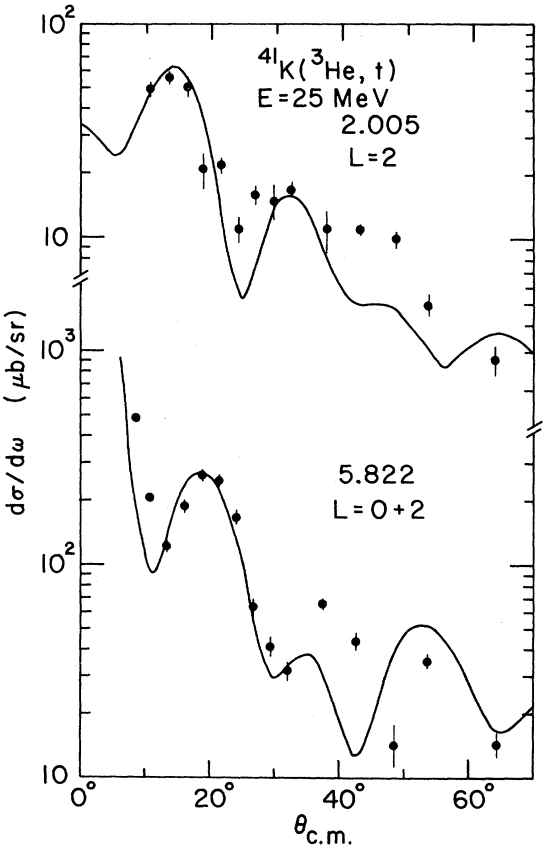

FIG. 7. Comparison of the 2.005- and 5.822-MeV angular distributions with DW calculations.

with spin-flip. However, Knöpfle *et al.*[3] have shown this configuration must be *very small* because there is no γ decay from the analog state to the 2.005-MeV state.

Another possibility is the $[d_{3/2}^{-1}(\frac{3}{2}, \frac{1}{2})f_{7/2}^2(2, 1)]_{(3/2,1/2)}$ configuration. This seems quite feasible since it can be reached by $L=2$ *without* spin-flip. In the (^{3}He, t) reaction one expects that states which do not involve spin-flip will be the most strongly excited. Evidence of this configuration can be found in other states of ^{41}Ca as well, as will be discussed in the next section.

In the ^{40}Ar(^{3}He, t) reaction[11] the analog state was characterized by $L=0$, while the antianalog state was characterized by $L=1$. This reaction is of particular interest here because the same transitions are required to reach the analog and antianalog states in ^{40}K and ^{41}Ca. The work of Schaeffer and Bertsch[13] show that this anomalous $L=1$ behavior can be explained by considering a pickup-stripping mechanism for the (^{3}He, t) reaction. Why then is the antianalog state in ^{41}Ca not observed with $L=1$? The answer can be found by observing the strengths of the cross sections. In ^{40}K the cross section of the analog state is about 25 times that of the antianalog state, while in the present study this factor is only about 6. Thus, one can argue that in ^{41}Ca the $L=1$ contribution due to the anti-analog configuration is small compared to the $L=2$ contribution due to a mixed configuration.

C. $\frac{1}{2}^+$ states at 2.68 and 3.39 MeV

Evidence about the character of the 2.68- and 3.39-MeV states has been obtained from several experiments. These states are observed in the ^{42}Ca(p, d) and ^{42}Ca(^{3}He, α) reactions[4,5] with $l_n=0$ resulting from the pickup of a $2s_{1/2}$ neutron. The 2.68-MeV state is strongly excited ($S=0.65$), while the 3.39-MeV state is only weakly excited ($S=0.12$). In the study of the ^{39}K(^{3}He, p) reaction by Belote *et al.*[7] the 3.39-MeV state was observed with 75% $L=0$ and 25% $L=2$ and the 2.68-MeV state was not observed. The γ-decay studies of Knöpfle *et al.*[3] show that the 3.39-MeV state must have a large contribution from the $[d_{3/2}^{-1}(\frac{3}{2}, \frac{1}{2})f_{7/2}^2(1, 0)]_{(3/2,\,1/2)}$ configuration, since the analog state decays directly to the 3.39-MeV state. These experiments and the shell-model calculations of Sartoris and Zamick[23] indicate that the wave functions for the $\frac{1}{2}^+$ states have the following form:

$$\begin{aligned}\psi_{(\frac{1}{2},\frac{1}{2})} = {} & A[s_{1/2}^{-1}(\tfrac{1}{2}, \tfrac{1}{2})f_{7/2}^2(0, 1)] \\ & + B[d_{3/2}^{-1}(\tfrac{3}{2}, \tfrac{1}{2})f_{7/2}^2(2, 1)] \\ & + C[d_{3/2}^{-1}(\tfrac{3}{2}, \tfrac{1}{2})f_{7/2}^2(1, 0)] \\ & + D[d_{3/2}^{-1}(\tfrac{3}{2}, \tfrac{1}{2})f_{7/2}f_{5/2}(1, 0)]. \qquad (1)\end{aligned}$$

The first term accounts for the pickup reactions, while the second and third terms account for the (^{3}He, p) reaction.[7]

In view of the results from the neutron pickup reactions one might expect that the 2.68-MeV state would be strongly excited in the ^{41}K(^{3}He, t) reaction, while the 3.39-MeV state would be only weakly excited. Therefore, one of the most striking features of the spectrum in Fig. 2 is that the state at 2.68 MeV is hardly excited, if at all, while the state at 3.39 MeV is moderately strong. At most, only traces of the 2.68-MeV state are evident, and then only at forward angles. The $L=2$ angular distribution for the 3.39-MeV state is shown in Fig. 8.

In the ^{41}K(^{3}He, t) reaction states with $J=\frac{1}{2}^+$ can be excited in several ways. An $s_{1/2}$ neutron can be replaced by a $d_{3/2}$ proton with $L=2$ corresponding to first term in Eq. (1). Also, an $f_{7/2}$ neutron can be replaced by an $f_{7/2}$ proton with $L=2$, corresponding to the second term in Eq. (1). The effect of the third term in Eq. (1) will be smaller because it requires spin-flip.

Distorted-wave calculations using program

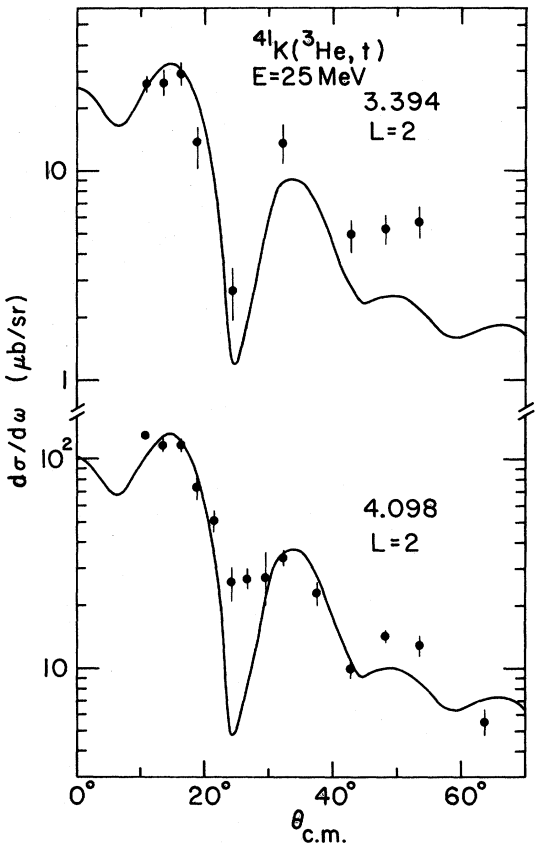

FIG. 8. Comparison of the 3.394- and 4.098-MeV angular distributions with DW calculations.

DWUCK show that the cross section for the $f_{7/2} \rightarrow f_{7/2}$ transition with $L = 2$ is about 5 times larger than for the $s_{1/2} \rightarrow d_{3/2}$ transition. Part of this effect is due to angular momentum algebra and part is due to the fact that the form factors for the two transitions are quite different. The form factor for the $s_{1/2} \rightarrow d_{3/2}$ transition has positive and negative parts due to the node in the $s_{1/2}$ wave function and none in the $d_{3/2}$ wave function. The form factor for the $f_{7/2} \rightarrow f_{7/2}$ transition is positive. The disparity is actually greater than a factor of 5 because there is only one vacancy in the $d_{3/2}$ proton shell, while the $f_{7/2}$ proton shell is vacant. Therefore, if the excitation of the 2.68- and 3.39-MeV states in the (^{3}He, t) reaction is due principally to the $f_{7/2} \rightarrow f_{7/2}$ transition, then the data for the (^{3}He, t) reaction indicate that the coefficient B in Eq. (1) is large for the 3.39-MeV state and small for the 2.68-MeV state. For example, if the two values of B differ by a factor of 3, then the cross sections will differ by a factor of 9. Such a reduction would make observation of the 2.68-MeV state very difficult. Furthermore, if the coefficients A and B have the same sign for the 3.39-MeV state, then in the orthogonal wave function for the 2.68-MeV state these coefficients may very well have opposite signs. If these two configurations interfere constructively for the 3.39-MeV state, then they would interfere destructively for the 2.68-MeV state. These arguments offer a reasonable explanation why the 2.68-MeV state was not observed in the (^{3}He, t) reaction.

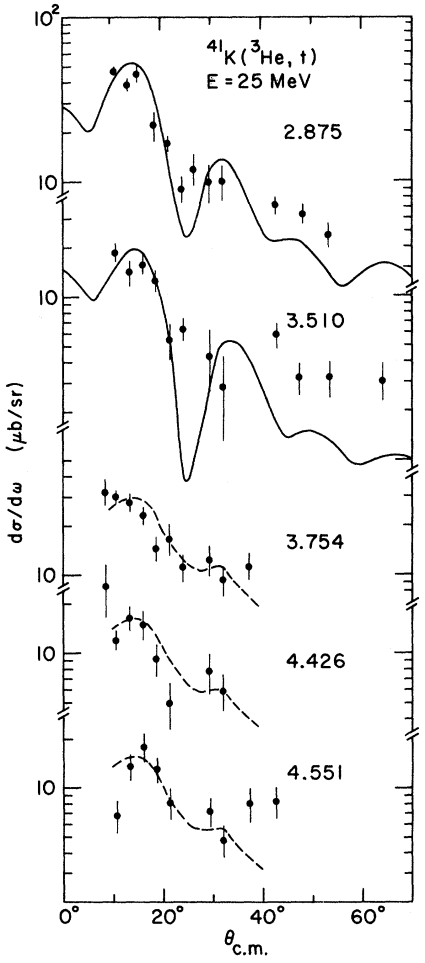

FIG. 9. The 2.875- and 3.510-MeV angular distributions are compared with $L = 2$ DW calculations. The dashed curve is explained in the caption of Fig. 10.

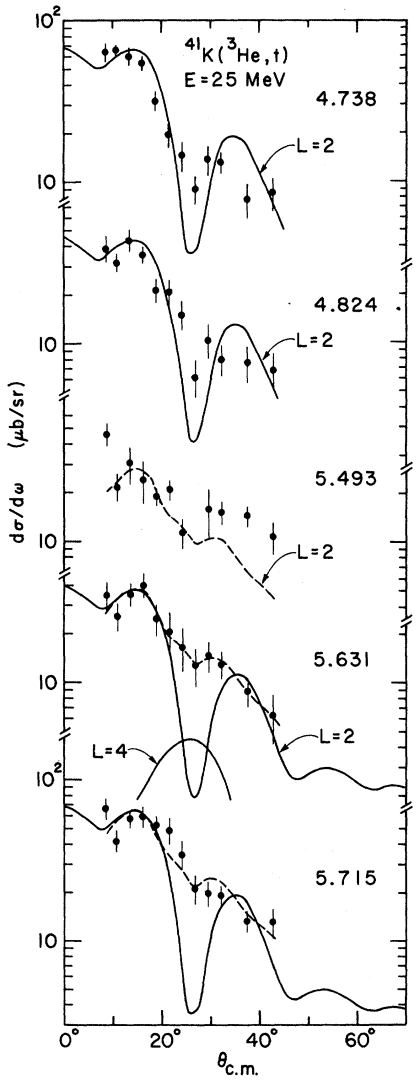

FIG. 10. The dashed curve is a visual fit through the data points of the 5.631-MeV angular distribution. It can be reproduced with DW calculations as described in the text. The solid-line curves result from DW calculations.

D. 4.098-MeV state

The state at 4.098 MeV has been assigned $J^\pi = \frac{5}{2}^+$ on the basis of a γ decay from this state to the $\frac{7}{2}^-$ ground state. The analog state at 5.813 MeV decays directly to the 4.098-MeV state, showing evidence for the $[d_{3/2}{}^{-1}(\frac{3}{2}, \frac{1}{2})f_{7/2}{}^2(1,0)]_{(5/2,\,1/2)}$ configuration.[3] The (^{3}He, p) reaction also shows a strong evidence for this configuration assignment; since $J^\pi = \frac{5}{2}^+$, the 90% $L=0$ transition must occur with $S=1$ and this configuration is the most likely due to the strong excitation of this state. In the (^{3}He, t) reaction, however, this configuration can only be reached with spin-flip. As discussed earlier, DW calculations which include the tensor force show that the cross section for $L=2$, $S=1$ dominates over $L=0$, $S=1$ for the $f_{7/2} \rightarrow f_{7/2}$ transition. Therefore, the angular distribution would be characterized by $L=2$, which is in agreement with the data shown in Fig. 8. However, an $L=2$ angular distribution can also be obtained with the $[d_{3/2}{}^{-1}(\frac{3}{2}, \frac{1}{2})f_{7/2}{}^2(2,1)]_{(5/2,\,1/2)}$ configuration. The

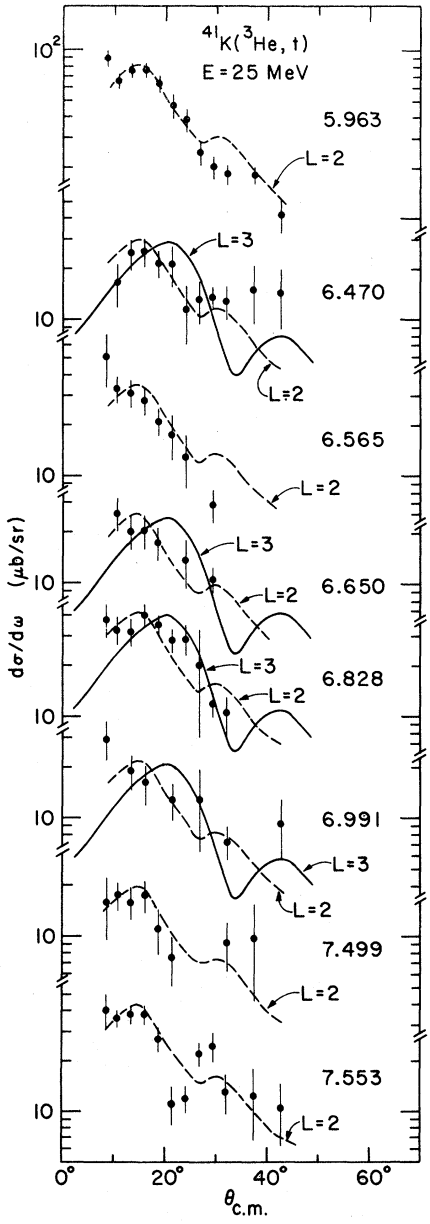

FIG. 11. Comparison of angular distributions with DW calculations.

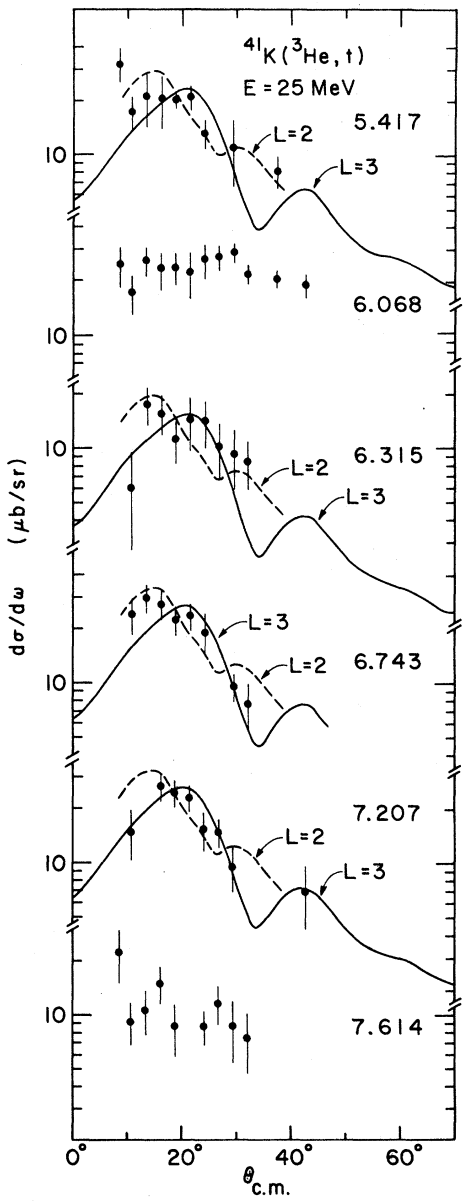

FIG. 12. Comparison of angular distributions with DW calculations.

strength of this configuration is smaller, because the $L=2$ transition in the $(^3\mathrm{He}, p)$ reaction occurs with only 10% probability. In the $(^3\mathrm{He}, t)$ reaction this configuration can be reached without spin-flip. Therefore, both configurations may enter into the excitation of this state. However, because spin-flip transitions are not excited as strongly as $S=0$ transitions, the $[d_{3/2}{}^{-1}(\frac{3}{2}, \frac{1}{2})f_{7/2}{}^2(2,1)]_{(5/2,\,1/2)}$ configuration may be largely responsible for the excitation of this state.

E. Other states

The rest of the angular distributions are compared with DW calculations in Figs. 9 thru 13. The results are summarized and compared with data from other reactions in Table II. Since all of the reactions have target nuclei with positive parity, then $(-)^{l_n}$ should equal $(-)^L$.

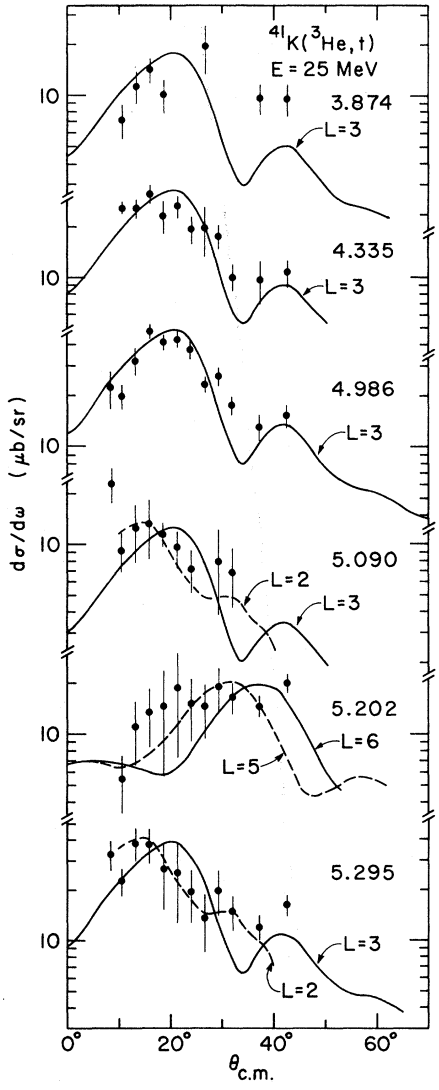

FIG. 13. Comparison of angular distributions with DW calculations.

2.875 MeV. In a recent study of the $^{40}\mathrm{Ca}(d,p)$ reaction,[24] the 2.875-MeV state (Fig. 9) was found to have $J^\pi = \frac{7}{2}^+$ or $\frac{9}{2}^+$. The present study confirms these results. Since $^{41}\mathrm{K}$ has $J^\pi = \frac{3}{2}^+$, $J^\pi = \frac{7}{2}^+$ can be obtained with $L=2$, $S=0$, while $J^\pi = \frac{9}{2}^+$ requires $L=2$, $S=1$. The $(^3\mathrm{He}, t)$ reaction may show a preference for the $J^\pi = \frac{7}{2}^+$ assignment, since $S=0$ transitions are more strongly excited than $S=1$ transitions.

5.631 MeV. The angular distribution for this state (Fig. 10) is characterized by $L=2$ between 8 and 20°, but a deep minimum at 25° is not found in the data. This may be due to an $L=4$ contribution, which peaks at this angle. In Fig. 10 the amount of $L=4$ contribution is shown relative to the $L=2$ contribution. Hence, when $L=2$ and $L=4$ contributions are included, the resultant curve is only slightly different from the $L=2$ curve. The dashed curve results if the $L=4$ contribution is increased by a factor of 3. The angular distributions of many states in Figs. 9 thru 13 are compared with the dashed curve and are considered indicative of $L=2$ with possibly some $L=4$ admixture. In contrast the data for the 2.875-, 4.738-, and 4.824-MeV states show a deep minimum at 25° and are fitted very well with $L=2$ DW calculations.

3.510 MeV. The angular distribution for the 3.510-MeV state (Fig. 9) has $L=2$. The transition to this state was found to have $l_n=2$ in the (p,d) reaction and $l_n=3$ in the $(^3\mathrm{He}, \alpha)$ reaction. Thus, the present study substantiates the $l_n=2$ assignment, and this state has $J^\pi = \frac{3}{2}^+$ or $\frac{5}{2}^+$.

4.824 MeV. The $L=2$ assignment for the angular distribution of the 4.824-MeV state (Fig. 10) is consistent with the positive parity for states at 4.817 and 4.829 MeV, which would not have been resolved in the present work.

4.986 MeV. The angular distribution for the state at 4.986 MeV (Fig. 13) is fitted extremely well with $L=3$. Therefore, it most likely corresponds with a state at 4.994 MeV rather than one at 4.983 MeV, which has positive parity.

5.090 MeV. The angular distribution for the 5.090-MeV state (Fig. 13) has $L=2$ or 3. In the $^{40}\mathrm{Ca}(d,p)$ reaction the transition to the 5.082-MeV state is characterized by $l_n=0$. This is in agreement with the $L=2$ assignment found in the $(^3\mathrm{He}, t)$ reaction. No spectroscopic information is known about the state at 5.107 MeV.

5.202 MeV. The angular distribution for the 5.202-MeV state (Fig. 13) has $L=5$ or 6 and is indicative of a high angular momentum transfer. A level was also seen at 5.208 MeV in the $^{40}\mathrm{Ca}(d,p)$ reaction, although l_n was not measured.

TABLE II. Summary of data and comparison with previous results.

E_x (MeV)	Error (keV)	This work L	This work J^π	Previous results [a] J^π	Previous results [a] E_x	(d, p) [b] l_n	$(^3\mathrm{He}, \alpha)$ [c] E_x	$(^3\mathrm{He}, \alpha)$ [c] l_n	$(^3\mathrm{He}, \alpha)$ [c] j	(p, d) [d] l_n
0		3+5	−	$\frac{7}{2}^-$	0	3	0	3	$\frac{7}{2}^-$	3
2.005	9	2	+	$\frac{3}{2}^+$	2.010	2	2.017	2	$\frac{3}{2}^+$	2
					2.680	0	2.680	0	$\frac{1}{2}^+$	0
2.875	12	2	$(\frac{7}{2}^+)$	+	2.881	4	2.887			
3.394	12	2	+	$\frac{1}{2}^+$	3.400	0	3.401	0	$\frac{1}{2}^+$	
3.510	12	2	$\frac{3}{2}^+$ or $\frac{5}{2}^+$		3.527		3.527	3	$\frac{7}{2}^-$	2
3.754	10	2	+	$(\frac{3}{2}, \frac{5}{2})^+$	3.738	2	3.749	2	$\frac{3}{2}^+$	
				$\frac{1}{2}^+$	3.845	0	3.862	0	$\frac{1}{2}^+$	0
3.874	10	(3)	(−)							
3.992	10				3.976 4.017					
4.098	8	2	+	$\frac{5}{2}^+$	4.091	ns [e]	4.108	3	$\frac{7}{2}^-$	2
4.335	9	3	−		4.332					
4.426	8	2	+		4.420					
4.551	11	(2)			4.549					
4.738	13	2	+	$(\frac{1}{2}, \frac{3}{2}, \frac{5}{2})^+$	4.731					
				$\frac{1}{2}^-$	4.753		4.742	1	$\frac{1}{2}^-$	
4.824	10	2	+	$(\frac{3}{2}, \frac{5}{2})^+$	4.817					
					4.829	2	4.832	2	$\frac{3}{2}^+$	2
				$(\frac{7}{2}, \frac{9}{2})^+$	4.971					
					4.983	4	4.986	4	$\frac{9}{2}^+$	
4.986	8	3	−		4.994					
					5.082	0				
5.090	15	2, 3			5.107					
5.202	10	5, 6			5.208					
5.295	7	2, 3			5.297	2	5.300	2	$\frac{3}{2}^+$	
5.417	7	2, 3			5.421		5.425	3	$\frac{7}{2}^-$	
5.493	10	(2)			5.493	1	5.505	3	$\frac{7}{2}^-$	
5.631	8	2	+		5.625					
					5.635					
5.715	10	2	+		5.714	1				
5.822	10	0	+	$\frac{3}{2}^+$	5.813		5.852	2	$\frac{3}{2}^+$	2
5.963	8	2	+		5.977		5.997	0	$\frac{1}{2}^+$	
6.068	8				6.070					
6.315	9	2, 3			6.311					
6.470	8	2, 3			6.468 6.473		6.472			
6.565	9	2	+		6.568	2	6.530			
6.650	9	2, 3			6.655					
6.743	8	2, 3								
6.828	7	2, 3		$\frac{1}{2}^+$	6.810 6.835		6.851	0	$\frac{1}{2}^+$	0
6.905	11						6.913			
6.991	9	2, 3					6.966	2	$(\frac{5}{2}^+)$	
7.120	11	3+5	−	$\frac{7}{2}^-$			7.173	3	$\frac{7}{2}^-$	3
7.207	14	2, 3								

TABLE II *(Continued)*

E_x (MeV)	Error (keV)	This work L	This work J^π	Previous results [a] J^π	Previous results [a] E_x	(d,p) [b] l_n	$(^3\mathrm{He},\alpha)$ [c] E_x	$(^3\mathrm{He},\alpha)$ [c] l_n	$(^3\mathrm{He},\alpha)$ [c] j	(p,d) [d] l_n
7.290	10						7.321	3		
7.499	8	2	+				7.539			
7.553	8	2								
7.614	8									

[a] A composite obtained from Refs. 2, 4, and 9.
[b] Reference 6.
[c] Reference 5.
[d] Reference 4.
[e] Nonstripping pattern.

5.295 MeV. The angular distribution for the 5.295-MeV state (Fig. 13) has $L=2$ or 3. However, the data from the pickup and stripping reactions show that $L=2$ must be correct.

5.493 MeV. The angular distribution for the 5.493-MeV state (Fig. 10) is tentatively assigned $L=2$. However, the transition to the state at 5.493 MeV has an $l_n=1$ assignment suggesting $\frac{1}{2}^-$ or $\frac{3}{2}^-$, while the transition to the state at 5.505 MeV has an $l_n=3$ assignment suggesting $\frac{5}{2}^-$ or $\frac{7}{2}^-$.

5.715 MeV. The angular distribution for the 5.715-MeV state (Fig. 10) has $L=2$. This is not in agreement with the $l_n=1$ transition to the state at 5.714 MeV.

Excited analog state at 6.828 MeV. The $\frac{1}{2}^+$ analog state was identified at 6.82 ± 0.05 MeV in the (p,d) reaction and at 6.851 MeV in the $(^3\mathrm{He},\alpha)$ reaction. In Fig. 11 the 6.828-MeV angular distribution is compared with $L=2$ and 3 DW calculations. However, since this state has $J^\pi=\frac{1}{2}^+$, L must equal 2.

ACKNOWLEDGMENTS

The authors would like to thank J. P. Schiffer for his assistance in the initial stages of this work and for helpful discussions. We would also like to acknowledge the discussions with M. H. Macfarlane concerning the antianalog states.

†Work performed under the auspices of the U.S. Atomic Energy Commission.
*Present address: Nuclear Structure Research Laboratory, University of Rochester, Rochester, New York 14627.

[1] J. R. Comfort, J. P. Schiffer, A. Richter, and M. M. Stautberg, Phys. Rev. Lett. 26, 1338 (1971).
[2] P. M. Endt and C. van der Leun, Nucl. Phys. A214, 1 (1973), and references therein.
[3] K. T. Knöpfle, M. Rogge, C. Mayer-Böricke, D. S. Gemmell, L. Meyer-Schützmeister, H. Ohnuma, and N. G. Puttaswamy, Phys. Rev. C 4, 818 (1971).
[4] S. M. Smith, A. M. Bernstein, and M. E. Rickey, Nucl. Phys. A113, 303 (1968).
[5] U. Lynen, R. Bock, R. Santo, and R. Stock, Phys. Lett. 25B, 9 (1967).
[6] T. A. Belote, A. Sperduto, and W. W. Buechner, Phys. Rev. 139, B80 (1965).
[7] T. A. Belote, F. T. Dao, W. E. Dorenbusch, S. Kuperus, J. Rapaport, and S. M. Smith, Nucl. Phys. A102, 462 (1967).
[8] J. J. Schwartz and B. A. Watson, Phys. Lett. 31B, 198 (1970).
[9] L. G. Elliott, Phys. Rev. 85, 942 (1952).
[10] L. R. Greenwood, J. C. Stoltzfus, K. Katori, C. P. Cameron, and T. H. Braid, Argonne Physics Division Informal Report No. PHY-1972B, 1972 (unpublished).
[11] R. A. Hinrichs, R. Sherr, G. M. Crawley, and I. Proctor, Phys. Rev. Lett. 25, 829 (1970).
[12] R. A. Hinrichs and G. F. Trentelman, Phys. Rev. C 4, 2079 (1971).
[13] R. Schaeffer and G. F. Bertsch, Phys. Lett. 38B, 159 (1972).
[14] M. Toyama, Phys. Lett. 38B, 147 (1972).
[15] T. A. Belote, H. Y. Chen, O. Hansen, and J. Rapaport, Phys. Rev. 142, 624 (1966).
[16] J. R. Comfort, Argonne National Laboratory Physics Division Informal Report No. PHY-1970B, 1970 (unpublished).
[17] P. D. Kunz (private communication).
[18] E. F. Gibson, B. W. Ridley, J. J. Kraushaar, M. E. Rickey, and R. H. Bassel, Phys. Rev. 155, 1194 (1967).
[19] J. C. Hafele, E. R. Flynn, and A. G. Blair, Phys. Rev. 155, 1238 (1967).
[20] E. Rost and P. D. Kunz, Phys. Lett. 30B, 231 (1969).
[21] P. Kossanyi-Demay, P. Roussel, H. Faraggi, and R. Schaeffer, Nucl. Phys. A148, 181 (1970).
[22] J. B. French and M. H. Macfarlane, Phys. Lett. 2, 255 (1962).
[23] G. Sartoris and L. Zamick, Phys. Rev. Lett. 18, 292 (1967).
[24] K. K. Seth, A. Saha, and L. Greenwood, Phys. Rev. Lett. 31, 552 (1973).